11TH INTERNATIONAL SYMPOSIUM FIELD MONITORING IN GEOMECHANICS

# Influence of reaction system on uplift behaviour of micropiles subjected to static pullout

Andreas-Nizar GRANITZER[1], Matthias J. REBHAN[1], Franz TSCHUCHNIGG[1]

[1]Graz University of Technology, Graz, Austria
Corresponding author: Andreas-Nizar Granitzer (andreas-nizar.granitzer@tugraz.at)

**Abstract**

Traditionally, static tension load tests are required to prove the suitability of piling systems, and to confirm the design parameters estimated from the site investigation. During the loading procedure the reaction system counteracts the upheaval movement of the tested pile resulting in an overestimation of both, the uplift bearing capacity and the pile stiffness. Although this phenomenon, referred to as bracing effect, is widely recognised by execution standards it still lacks physical evidence. In this context, the present contribution focuses on the mutual interaction between the reaction system and test pile with particular emphasis on micropiles. The presented study has been partly carried out in the scope of the research project "Durability in Anchor Technique" (DAT), and involves both full-scale field tests as well as numerical studies based on validated models. The results showcase the bracing effect on the monitored micropile response, albeit being considerably reduced compared to previous studies concerning static load tests of large diameter piles; this observation supports the exception clauses of many execution standards that alleviate the geometrical requirements for load testing of micropiles. Since the bracing effect is pronounced in the near surface, the response of short micropiles is expected to be particularly prone to mutual locking. Consequently, future work should focus on its role during static loading of short micropiles with low slenderness ratio.

Keywords: micropile, pullout, bracing effect, field test, embedded beam.

## 1. Introduction

Since micropiles are especially suited for projects with restricted clearance, difficult access, and poor ground conditions, they offer a wide range of geo-engineering applications. Starting with their first introduction in the 1950s (Lizzi 1964), micropiles are being used for various purposes of reinforcing foundations, underpinning existing structures, improving ground conditions, and enhancing the seismic performance (FHWA 2005; Tsukada et al, 2006; Esmaeili et al, 2013). Given their ease of installation, they are increasingly utilized as integral part of rockfall protection systems; in combination with special energy absorbing elements at the interplay with steel ropes, they improve the energy dissipation capabilities and ensure a high flexibility in the protection from natural hazards. In many instances, these micropiles have to be installed in steep terrain with limited access which requires considerable effort in the execution of static tension load tests according to the European standard prEN ISO 22477-2 (2022).

In order to enable the execution of field-tests, the measurement equipment is commonly placed on reaction frames comprising steel beams; see Figure 1a. Unlike compression piles that may be regarded as standard reaction device in almost horizontal terrain, this type of reaction system produces particularly high stress concentrations in subsoil regions surrounding the test pile in the near surface. In both, research and practice, there exists consensus about the mutual influence between the test pile and the reaction device during static pile load tests (Poulos and Davis 1980; Kitiyodom et al, 2004; Latotzke et al, 1999; Comodromos et al, 2003; Weltman 1980). With regard to static pullout testing, the reaction forces counteract the upheaval movement of the test piles giving rise to spurious estimates of the individual pile performance. In the following, this source of misinterpretation is referred to as bracing effect. As a consequence, the measurements tend to indicate a too stiff response and an overestimation of the pullout capacity. This effect decreases with increasing clear distance (CD) between the reaction device and the micropile.

Although this interaction has been recognized by various standards, its intensity and significance in the interpretation of pile load tests is not completely understood. As a consequence, current guidelines concerning minimum CD thresholds between the reaction device and the test pile (MCD) differ considerably; see Table 1. Moreover, the majority of guidelines focuses on static compression load testing of large diameter piles, and does not provide specifications regarding pile length, soil conditions and reaction device type. From the above discussion, it can be concluded that the determination of a reliable MCD is still a delicate issue, prompting the question as which MCD should be selected to verify the reliability of pile supported structures with sufficient accuracy.

The present paper aims at serving as practical reference to engineers that have to assess the influence of the reaction frame on the micropile response during static tension load tests. Section 2 is devoted to an instrumented micropile pullout test; in an attempt to monitor the development of shaft normal forces at different depths, the micropile is installed with a secondary measuring system, in addition to the standard instrumentation required for monitoring the global pile response.

| Literature source | ONR 24810 (2020) | (DGGT 2013) | prEN ISO 22477-2 (2022) | (Fleming et al. 2009) |
|---|---|---|---|---|
| MCD | $5 \cdot D_{pile}$ | 1.5 m | $3.5 \cdot D_{pile}$ \| 2.5 m | $5 \cdot D_{pile}$ ($3\text{-}4 \cdot D_{pile}$) |
| Loading type | Tension | Compression | Tension | Compression |
| Reaction device | Shallow foundation | Tension piles, kentledge support | Compression piles, shallow foundation | Tension piles |
| Miscellaneous | Rock mass embedment may reduce MCD. | MCD shall prevent bracing in micropile tensile load tests. | MCD may be reduced to 1.5 m for micropiles. | Bracing effect shall be limited to 20 % of pile settlements. |

**Table 1**: Minimum clear distance (MCD) between centres of test pile and types of reaction device.

In section 3 and 4, numerical simulations are presented with the aim to investigate the bracing effect in more detail. As part of the research project, the numerical model is validated with the recorded field test data. The calibrated numerical model is used to analyse the influence of the CD on different aspects of the bracing effect such as the mobilization of shaft normal stresses, uplift capacity and failure mechanism. Section 5 closes with the main conclusions of this work.

**2. Micropile Tension Load Test**

As part of the research project "DAT" (Rebhan et al, 2022), an instrumented field test has been carried out in the area of Graz at the test field "Inffeldgasse", the latter being situated on the campus of the Graz University of Technology in Graz, Austria. The soil profile is determined based on the results of a geotechnical investigation including two standard penetration tests, three 15 m boreholes, and laboratory tests on samples taken using shelby tubes. The soil stratification is composed of two layers. The upper layer is dominated by backfill material down to -2.5 m, underlying alluvial Quaternary sandy gravels, locally known as "Murschotter". The ground water has not been encountered in the deepest boring.

The investigated micropile with a nominal length of 4 m is designed as GEWI-pile with standard corrosion protection. The load-bearing element is formed by a SAS 550 thread bar system with a diameter $D_{bar}$ = 32 mm, and is installed using the percussive drilling technique with temporary casing and a lost bit. Grouting is realised by means of gravity filling, conforming to micropile type A1 of the classification scheme documented in FHWA (2005). As shown in Figure 1a, the reaction system is composed of two UPE 240x50 type spreader beams supported on two pairs of UPE 160x50 reaction beams forming the reaction device. In accordance with the Austrian standard ONR 24810 (2020) CD = $5 \cdot D_{pile}$ = 0.62 cm. The vertical displacements of both, the pile head and the reaction frame are monitored by a data acquisition system including displacement transducers and draw-wire sensors. The measuring devices are fixed on rigid reference entities that are supported at points placed far enough from the test area to eliminate any interaction effects. The hydraulic pressure in the jacking system is controlled through a load cell.

In order to analyse the evolution of the bracing effect in the near surface, the uppermost bar segment is equipped with two custom-made load cells at a depth of -0.5 m (Ro) and -1.3 m (Ru). As can be seen in Figure 1b, these load cells are locally fixed by means of connection sleeves. However, due to problems in the recording of the input signal generated by the lower load cell (Ru) caused by an installation malfunction, only the upper load cell (Ro) is considered in the evaluation of the bracing effect. The grout level is limited to a depth of -1.5 m. This allows for the coupling of the instrumented bar segment after drilling to the final depth; the residual borehole length is temporary supported by a PVC pipe, and subsequently backfilled with compacted sand. In the absence of a grout-to-ground interface, the sectional bond capacity is substantially impaired along the backfilled length, and therefore assumed as unbonded in the numerical simulations presented in section 3 and 4.

Prior to the execution of the uplift test, the piling platform level is reprofiled using an excavator in combination with compacted sand. During the maintained pullout test particular emphasis is placed on the careful specification of loading increments and the time periods for which these increments are held constant; Figure 1c shows the recorded load step sequence. Due to the nature of the problem, the test micropile and the reaction

device are simultaneously loaded with the same vertical load magnitude ($F_v$) pointing in the opposite vertical direction. The maximum evaluated value of the tensile resistance is around 125 kN. As could be expected, the horizontal cell load ($F_h$) measured in the perpendicular direction of the micropile axis yields considerably lower magnitudes, but indicates a similar trend compared to the vertical pile load during the first stage of loading. This is a clear indication of an interaction between the reaction device and the test micropile at shallow depths. In contrast, $F_h$ gives almost constant values at higher test load levels ($F_v$ > 80 kN). This is partly attributed to the gradual formation of plastic zones between the reaction device and the test. From a practical point of view, this indicates that the influence of the reaction system on the micropile response decreases with increasing $F_v$.

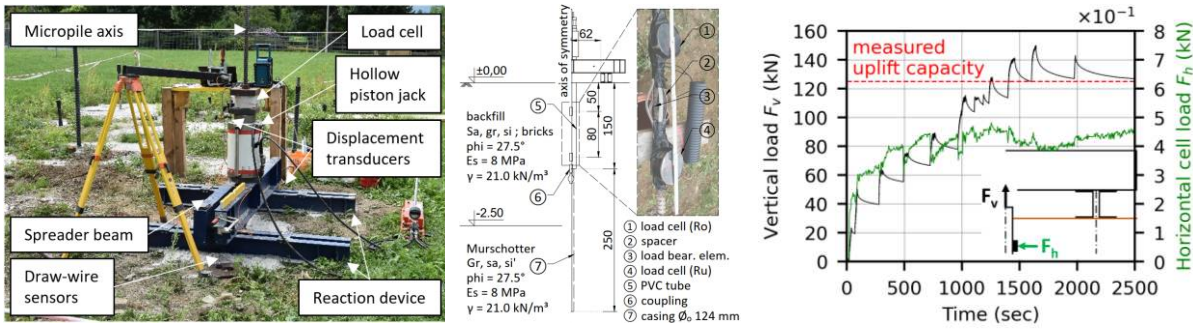


(a) (b) (c)

**Figure 1**: (a) Load test arrangement, (b) micropile instrumentation and (c) measured load-displacement curves.

To examine the bracing effect on the observed micropile response in more detail, the field test is numerically extended to varying CD. The analysis performed for this purpose is based on modelling assumptions which are verified through a back-analysis of the micropile test results.

### 3. Back-analysis – Simulation of the Pullout Test

In the investigation of the bracing effect induced by the reaction device in the area around the test micropile the field test is extended using comparative finite element analyses (FEA) with varying CD. The FEA carried out for this purpose are validated based on the vertical displacements of both the micropile head and the reaction frame measured during in-situ pullout testing. This ensures the overall resemblance of field measurements while preserving identical boundary conditions during parametric FEA, the latter being far from warranted in a field test series (Latotzke et al, 1999). The uplift test configuration is numerically investigated using the finite element code Plaxis 3D (Bentley 2022) adopting the Updated Lagrangian formulation (Augarde et al, 2021). Based on the results of trial calculations the model domain is defined such that boundary effects are reduced to an acceptable limit. In this respect, Figure 2a specifies the model geometry, together with the mesh discretization composed of around 140.000 quadratic tetrahedral elements.

The applied Dirichlet boundary conditions (BC) prevent movements in the direction normal to the lateral model boundaries and in all coordinate directions (X, Y, Z) at the model base (Z = -12 m). Due to the symmetrical nature of the problem only one quarter of the problem is considered; the planes of symmetry (PoS) at Y, X = 0 m require that the displacements in the lateral direction are set to zero over this plane. Likewise, respective rotational degrees of freedom are constrained to zero at the plate element nodes located along the PoS. UPE steel profiles with parallel flanges and linear elastic material behaviour representing reaction system components are explicitly modelled by means of Reissner-Mindlin plate elements (Bathe 1982) with equivalent material properties and rigid connections. The soil stratification characterized in Figure 1b is typical for sites in the centre of Graz in the vicinity of the Mur river. This allows to adopt the constitutive parameters of the Hardening Soil Small (HSS) model with non-associated flow rule and small-strain stiffness overlay (Benz *et al.* 2009) from documented research projects executed at the Institute of Soil Mechanics, Foundation Engineering and Computational Geotechnics in Graz; for example, see Račanský (2008).

In view of the micropile modelling, two numerical simulation strategies are employed; namely, the widely accepted standard FE approach (SFEA) (Tschuchnigg and Schweiger 2015), an assembly of 3D solid elements with zero-thickness interface elements (van Langen and Vermeer 1991; Potts and Zdravković 1999), and the novel embedded beam element with interaction surface (EB-I) (Granitzer and Tschuchnigg 2021). The micropiles are idealised as linear elastic isotropic material with a Coulomb friction model at the interaction surface; in this context, the equivalent Young's modulus (Ẽ) is determined by means of the equivalent area method (Kyung and Lee 2017) which implies compatibility of axial deformation between the steel reinforcement and the grout

matrix along the loading direction. As the pullout test has been undertaken several weeks after the micropile installation, the grout is assumed cured at the time of loading; hence, no time dependency of the grout material is considered. With regard to small-strain FEA of similar problems, several attempts have been made to account for an increase of horizontal stresses due to lateral movements in the soil during installation and gravity grouting, both leading to an increase in shaft friction and pile stiffness (Schmüdderich et al, 2020; Fabris et al, 2021). Notably, these approaches require simplifying assumptions to mimic the state variation induced in the ground that are still under debate. In an attempt to capture the monitored system response with high accuracy, a semi-empirical modelling technique is adopted to account for the increase of lateral stresses along the bond zone, similar to Fabris et al, (2021). Consequently, this effect is considered by increasing the coefficient of lateral earth pressure ($K_0$) to 2.3 along the micropile bond length. This is an approximation based on literature (Littlejohn 1980) and experience acquired from comparable soil-structure interaction problems.

The simulation sequence includes an initial step in which the initial stress conditions are established, followed by the successive activation of the micropile and reaction system sub-domains, respectively. Simultaneous loading of the reaction frame (RF) and the micropile is simulated by imposing uniform increments of vertical Neumann BCs ($F_{v,inc.}$ = 20 kN related to the reduced geometry) along the model axis until the uplift failure threshold is reached. Figure 2b compares the predicted load-displacement curves with the field test results demonstrating remarkable agreement. This holds true for both micropile modelling approaches.

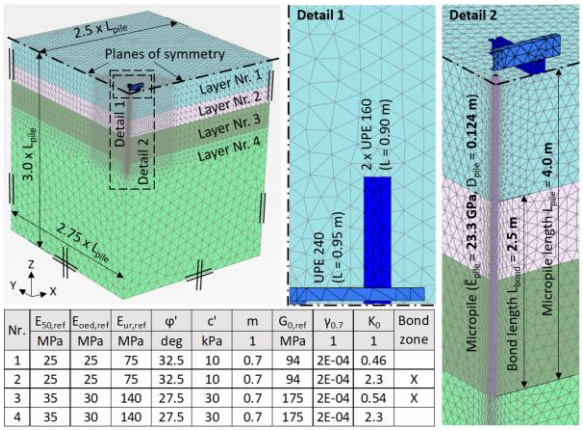


| Nr. | $E_{50,ref}$ | $E_{oed,ref}$ | $E_{ur,ref}$ | φ' | c' | m | $G_{0,ref}$ | $\gamma_{0.7}$ | $K_0$ | Bond zone |
|---|---|---|---|---|---|---|---|---|---|---|
| | MPa | MPa | MPa | deg | kPa | 1 | MPa | 1 | 1 | |
| 1 | 25 | 25 | 75 | 32.5 | 10 | 0.7 | 94 | 2E-04 | 0.46 | |
| 2 | 25 | 25 | 75 | 32.5 | 10 | 0.7 | 94 | 2E-04 | 2.3 | X |
| 3 | 35 | 30 | 140 | 27.5 | 30 | 0.7 | 175 | 2E-04 | 0.54 | X |
| 4 | 35 | 30 | 140 | 27.5 | 30 | 0.7 | 175 | 2E-04 | 2.3 | |

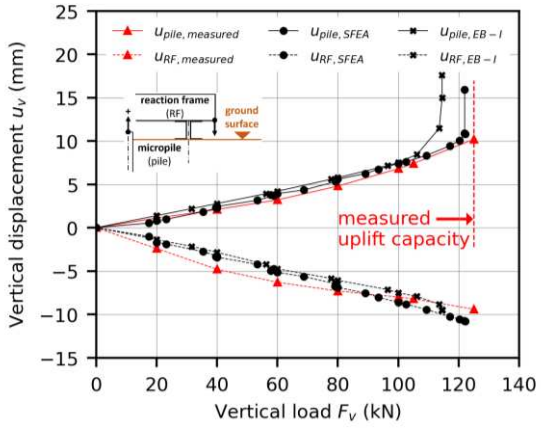


(a) (b)

**Figure 2**: (a) Geometry and mesh discretization (SFEA); (b) validation against load-displacement recordings.

The comparative study presented in section 4 partly concerns the evolution of normal stresses along the soil-micropile interaction surface imposed by mutual locking effects between the reaction frame and the micropile. To the authors' knowledge, the implicit interface formulation implemented with the EB-I has been thoroughly validated in terms of axial loading in vertical direction (Granitzer and Tschuchnigg 2021); in contrast to the SFEA, however, its suitability in the prediction of the stress field perpendicular to the EB-I axis is still under debate. As this research question is beyond the scope of this work, the parametric FEA are restricted to the SFEA pile model.

**4. Parametric Study**

To provide further insight into the role of the bracing effect during static micropile pullout tests, the validated model is studied with CD-values varying between $3 \cdot D_{pile}$ and $15 \cdot D_{pile}$. The selected values implicitly involve the range of MCD thresholds documented in well-established specifications for the execution of static pile load tests; see Table 1. In an additional simulation, the micropile is subjected to a static tension load without consideration of the reaction system. The latter is referred to as single pile model (SPM) and serves as reference to quantify effects imposed by the load transfer through the reaction system components.

As can be observed from Figure 3a, the uplift force-displacement relationships obtained adopting the reaction system models (RSM) and the SPM are almost identical in the initial stage of loading. In all cases considered, the micropile stiffness gradually decays with increasing upward movement which is attributed to the gradual mobilization of shear resistance along the micropile shaft. As it could be expected, the influence of the reaction system leads to a stiffer micropile response at higher load levels. More specifically, the slope inclination of the uplift force-displacement curve increases with decreasing CD; however, the results appear practically insensitive to the influence of the reaction system at working load conditions.

Figure 3b concerns the effect of the reaction system on the calculated tensile resistance at the ultimate limit state, shown by plotting the influence factor $f$ versus the CD-magnitude:

$$f = \frac{R_{RS} - R_{single\ pile}}{R_{single\ pile}} \cdot 100\% \quad (1)$$

In the Equ. 1, $R_{RS}$ and $R_{single\ pile}$ are the calculated tensile resistance values at the ultimate limit state obtained with RSM and SPM, respectively. The numerical predictions show an almost bi-linear distribution with a steeper inclination for CD < 5·$D_{pile}$, whereas the upper bound of $f$ stays below 10 %. Notably, this value is significantly lower compared to peak results derived from centrifuge experiments on low-aspect-ratio test piles ($L_{pile}/D_{pile} = 7$) subjected to static compression (Latotzke et al, 1999). Otherwise, $f$-values remain almost constant for RF models where CD < 5·$D_{pile}$. In view of the practical demand to keep CD small, given the obstacles during field tests (Fleming et al. 2009), the limit criterion according ONR 24810 (2020) (i.e. MCD ≥ 5·$D_{pile}$) appears reasonable to restrict the overestimation of the tensile resistance to approximately 5 % as required by ISO 22477-2 (2022)

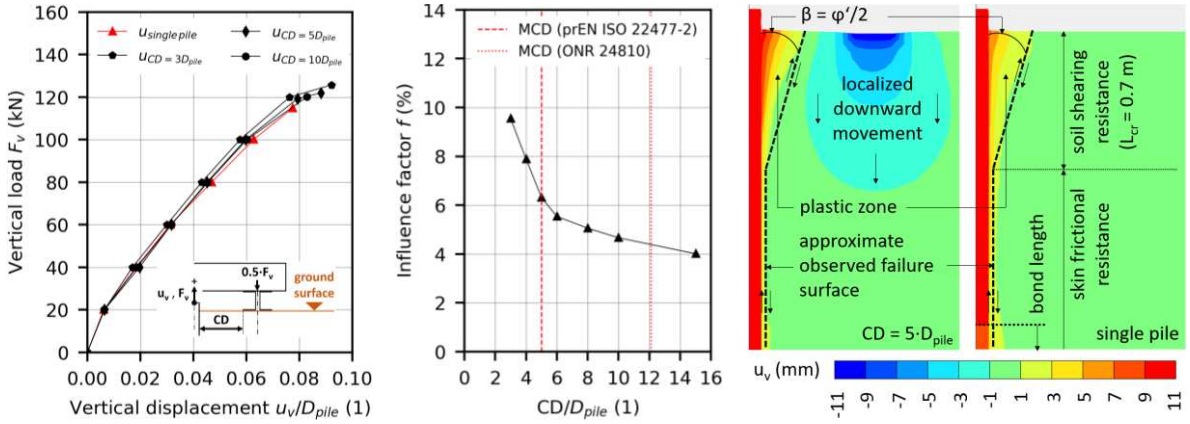


(a) (b) (c)

**Figure 3:** (a) Influence of clear distance (CD) between micropile and reaction system on load-displacement behaviour; (b) influence factor $f$ as function of the normalized CD; (c) failure mechanism (CD = 5·$D_{pile}$).

Figure 3c indicates the failure mechanisms by means of the vertical displacement contours evaluated at the final converged increment of the FEA before failure. Unlike the SPM, the RSM predicts significant settlement concentrations close to the reaction device. However, in all cases considered the observed failure surface is well approximated by a bi-linear boundary separating soil regions of different displacement magnitude despite the presence of the reaction frame in the RSM; herein, high-displacement regions inside the failure surface are referred to as plastic zone. To a depth of 0.7 m the inclination of the failure surface β is roughly represented by an angle of φ'/2 with respect to the vertical axis. Below the so-called critical embedded depth $L_{cr}$, the failure surface is aligned with the soil-grout shear boundary. It is noted that these observations are confirmed by experimental studies focusing on uplift capacity tests (Hong and Chim 2015). With regard to the load transfer mechanism, the uplift resistance is mobilized by the combination of the soil shearing resistance along the critical embedded depth $L_{cr}$, and the skin frictional resistance along the residual micropile length.

The normal stresses acting in perpendicular direction to the shaft play a major factor in the mobilization of the pullout capacity (Hong and Chim 2015). In common practice, they are regarded constant along the test micropile circumference despite apparent bracing effects. This assumption is disproved by Figure 4 where the angular distribution of the normal stress ratio (NSR) $\sigma'_{n,RS}$ / $\sigma'_{n,single\ pile}$ around the micropile circumference is illustrated at different micropile cross-section (Z ∈ {0.5, 1.0, 2.0} m); for reasons of consistency, $F_v$ = 100 kN < uplift capacity is considered as reference load level in the analysis. At a pile depth of 0.5 m, the normal stress ratio shows an asymmetrical distribution with increasing magnitude towards lower CD-values. As could be expected, the maximum NSR = 2.6 occurs at the x-axis intersection point where the horizontal distance between the micropile and the reaction system is equal to CD. In contrast, NSR-values are almost symmetrically deployed at a micropile depth of 1.0 m where the maximum NSR reduces to 2.1. In contrast to the above cross-sections, the lowermost cross-section intersects the bond zone at Z = -2.0 m. At this position, NSR-magnitudes reduce to a constant value of 1.0 indicating single pile stress conditions. This underlines the subordinate importance of the bracing effects along the majority of the bond length.

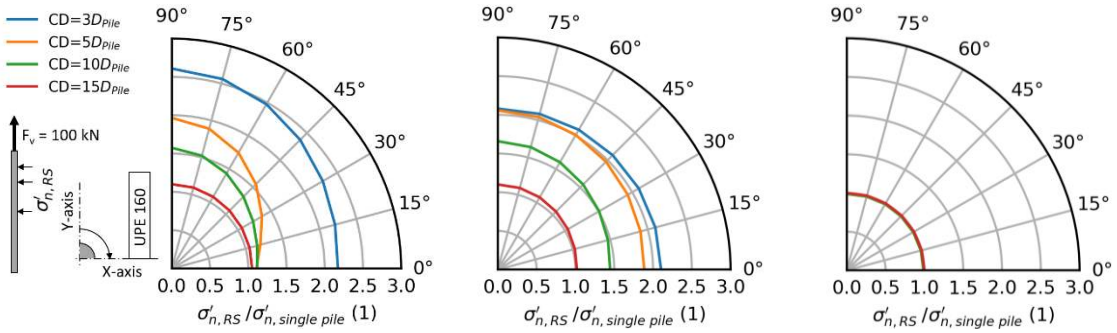


**Figure 4:** Distribution of interface normal stress ratio at Z-coordinates (a) -0.5 m, (b) -1.0 m and (c) -2.0 m.

It is of great importance to notice that the investigations presented in this paper are restricted to micropile configurations where $L_{pile}$ is significantly greater than the critical embedment depth $L_{cr}$ (Figure 3c). In cases with short micropile lengths and a strong micropile-soil interface, it is conceivable that pullout may involve heaving of the ground surface with surface breakout (Kulhawy 1985). This may alter the influence of the bracing effect on micropiles during static tension load testing, and should be studied in future research.

## 5. Conclusions

The mutual interaction between micropiles and reaction systems during static tension load tests represents a complicated phenomenon that is still not fully understood. In an attempt to acquire more detailed insight, a full-scale micropile pullout test is conducted in coarse-grained subsurface conditions. In addition to the standard instrumentation for monitoring its global load bearing behaviour, the micropile is instrumented with a secondary measuring system which allows for the monitoring of shaft normal forces in the radial direction during the testing procedure. Although restricted to a qualitative assessment of the bracing effect, the measurements showcase the expected trend of an increase in shaft normal force with test load level in the initial stage of loading. At test load levels close to the ultimate limit state, however, the measured shaft normal force remains practically constant.

The full-scale field test is numerically back-calculated using geometrically non-linear FEA. The validated model serves as starting point for a parametric study on the role of the CD during static pullout tests. In all cases considered, the micropile stiffness is practically insensitive to varying CD. With regard to the tensile resistance at the ultimate limit state, the single pile response is overestimated by less than 10 % due to the influence of the reaction system. To restrict bracing effects to an acceptable limit on the one hand, and satisfy the practical need for low CD-values on the other hand, the numerical results suggest MCD $\geq 5 \cdot D_{pile}$ as practicable limit criterion, which complies with the specifications documented in the Austrian standard ONR 24810 (2020).

In addition, a detailed analysis of the cross-section interface normal stress distribution confirms that the bracing effect on the micropile response decreases with increasing depth. This implies that short micropiles with a low slenderness ratio are particularly prone to bracing effects. In order to define generally applicable MCD limit criterions, future work should therefore concentrate on parameter studies with varying $L_{pile}$ and subsurface conditions. In view of the pile modelling technique, future research may also concern the evaluation of suitable penalty stiffness magnitudes governing the coupling between the EB-I and the surrounding soil.

## Acknowledgements

The field test presented in this paper has been implemented in the course of the research project “DAT” (Durability in Anchor Technique) funded by the Austrian Research Promotion Agency FFG. Special thanks are also given to the R&D unit of Bentley Systems in Delft for their valuable support in the development of the EB-I.

## References

Augarde, C.E., Lee, S.J., and Loukidis, D., 2021. Numerical modelling of large deformation problems in geotechnical engineering: A state-of-the-art review. *Soils and Foundations,* 61 (6), 1718–1735.

Bathe, K.-J., 1982. *Finite element procedures in engineering analysis*. Englewood Cliffs, N.J.: Prentice-Hall.

Bentley, 2022. *Reference Manual. Plaxis 3D CE V22.00*.

Benz, T., et al., 2009. Small-strain stiffness in geotechnical analyses. *Bautechnik,* 86 (1), 16–27.

Comodromos, E.M., Anagnostopoulos, C.T., and Georgiadis, M.K., 2003. Numerical assessment of axial pile group response based on load test. *Computers and Geotechnics,* 30 (6), 505–515.

DGGT, 2013. *Recommendations on Piling. (EA-Pfähle)*. Berlin, Germany: Wiley.

Esmaeili, M., Nik, M.G., and Khayyer, F., 2013. Experimental and Numerical Study of Micropiles to Reinforce High Railway Embankments. *International Journal of Geomechanics,* 13 (6), 729–744.

Fabris, C*., et al.,* 2021. Numerical Simulation of a Ground Anchor Pullout Test Monitored with Fiber Optic Sensors. *Journal of Geotechnical and Geoenvironmental Engineering,* 147 (2), 1–10.

FHWA, 2005. *Micropile Design and Construction Reference Manual*. Washington, D.C.

Fleming, K*., et al.,* 2009. *Piling engineering*. 3rd ed. UK, London: Taylor & Francis.

Granitzer, A.-N., and Tschuchnigg, F., 2021. Practice-Oriented Validation of Embedded Beam Formulations in Geotechnical Engineering. *Processes,* 9 (10), 1739.

Hong, W.-P., and Chim, N., 2015. Prediction of uplift capacity of a micropile embedded in soil. *KSCE Journal of Civil Engineering,* 19 (1), 116–126.

Kitiyodom, P., Matsumoto, T., and Kanefusa, N., 2004. Influence of reaction piles on the behaviour of a test pile in static load testing. *Canadian Geotechnical Journal,* 41 (3), 408–420.

Kulhawy, F.H., 1985. Uplift behavior of shallow soil anchors - An overview. *In:* S. Clemence, ed. 1985. Detroit, USA, 1–25.

Kyung, D., and Lee, J., 2017. Uplift Load-Carrying Capacity of Single and Group Micropiles Installed with Inclined Conditions. *Journal of Geotechnical and Geoenvironmental Engineering,* 143 (8), 1–10.

Latotzke, J., König, D., and Jessberger, H.L., 1999. Effects of reaction piles in axial pile tests. *In:* ICSMFE, ed. 14th International Conference on Soil Mechanics and Foundation Engineering.

Littlejohn, G.S., 1980. Design estimation of the ultimate load-holding capacity of ground anchors. *Ground Engineering,* 13 (8), 25–39.

Lizzi, F., 1964. Root pattern piles underpinning. *In:* Central Building Research Institute, ed. Symposium on Bearing Capacity of Piles 1964, 305–320.

ONR 24810: 2020. Technischer Steinschlagschutz — Begriffe, Einwirkungen, Bemessung und konstruktive Durchbildung, Überwachung und Instandhaltung.

Potts, D.M., and Zdravković, L., 1999. *Finite element analysis in geotechnical engineering. Theory*. UK, London: Thomas Telford.

Poulos, H.G., and Davis, E.H., 1980. *Pile Foundation and Design*. USA, New York: Wiley.

prEN ISO 22477-2: 2022. Geotechnical investigation and testing - Testing of geotechnical structures. Part 2: Testing of piles: Static tension load testing.

Račanský, V., 2008. *Design of jet grout structures.* PhD Thesis: Brno University of Technology.

Rebhan, M.J*., et al.,* 2022. Dauerhaftigkeit von Mikropfählen und anderen Verankerungselementen. *In:* ÖIAV, ed. 13. Österreichische Geotechniktagung, 113–124.

Schmüdderich, C*., et al.,* 2020. Strategies for numerical simulation of cast-in-place piles under axial loading. *Computers and Geotechnics,* 125, 1–19.

Tschuchnigg, F., and Schweiger, H.F., 2015. The embedded pile concept – Verification of an efficient tool for modelling complex deep foundations. *Computers and Geotechnics,* 63, 244–254.

Tsukada, Y*., et al.,* 2006. Mechanism of Bearing Capacity of Spread Footings Reinforced with Micropiles. *Soils and Foundations,* 46 (3), 367–376.

van Langen, H., and Vermeer, P.A., 1991. Interface elements for singular plasticity points. *International Journal for Numerical and Analytical Methods in Geomechanics,* 15 (5), 301–315.

Weltman, A.J., 1980. *Pile load testing procedures*. UK, London: Directorate of Civil Engineering Services, Property Services Agency, Construction Industry Research and Information Association.